How Can (−)-Epigallocatechin Gallate from Green Tea Prevent HIV-1 Infection.Mechanistic Insights from Computational Modeling and the Implication for Rational Design of Anti-HIV-1 E...

ARTICLE *in* THE JOURNAL OF PHYSICAL CHEMISTRY B · MARCH 2006

Impact Factor: 3.3 · DOI: 10.1021/jp0550762 · Source: PubMed

2 AUTHORS, INCLUDING:

Adel Hamza
University of Kentucky
72 PUBLICATIONS **1,094** CITATIONS

SEE PROFILE

How Can (−)-Epigallocatechin Gallate from Green Tea Prevent HIV-1 Infection? Mechanistic Insights from Computational Modeling and the Implication for Rational Design of Anti-HIV-1 Entry Inhibitors

Adel Hamza* and Chang-Guo Zhan*

Department of Pharmaceutical Sciences, College of Pharmacy, University of Kentucky, 725 Rose Street, Lexington, Kentucky 40536

Received: September 8, 2005; In Final Form: December 14, 2005

Possible inhibitors preventing human immunodeficiency virus type 1 (HIV-1) entry into the cells are recognized as hopeful next-generation anti-HIV-1 drugs. It is highly desirable to develop a potent inhibitor blocking binding of glycoprotein CD4 of the cell with glycoprotein gp120 of HIV-1, because the gp120−CD4 binding is the initial step of HIV-1 entry into the cells. It has been recently reported that (−)-epigallocatechin gallate (EGCG) from green tea is an inhibitor blocking gp120−CD4 binding. But the inhibitory mechanism remains unknown. For understanding the inhibitory mechanism, extensive molecular docking, molecular dynamics simulations, and binding free-energy calculations have been performed in this study to predict the most favorable structures of CD4−EGCG, gp120−CD4, and gp120−CD4−EGCG binding complexes in water. The results reveal that EGCG binds with CD4 in such a way that the calculated binding affinity of gp120 with the CD4−EGCG complex is negligible. So, the favorable binding of EGCG with CD4 can effectively block gp120−CD4 binding. The calculated CD4−EGCG binding affinity ($\Delta G_{bind} = -5.5$ kcal/mol, $K_d = 94$ μM) is in excellent agreement with available experimental data suggesting $IC_{50} \approx 100$ μM for EGCG-blocking CD4−gp120 binding. These results and insights provide a rational basis for future design of novel, more potent inhibitors to block gp120−CD4 binding.

Introduction

Human immunodeficiency virus type 1 (HIV-1) continues to be the main cause for acquired immunodeficiency syndrome (AIDS) infection affecting millions of lives every year. More than 42 million people worldwide have been infected with HIV/AIDS, and in 2003 alone, more than three million, including 610 000 children, died from AIDS.[1] Of the 42 million infected, 6 million are in urgent need of antiretroviral (ARV) treatment to save their lives. HIV-1 encodes three enzymes that are essential for virus replication: reverse transcriptase, protease, and integrase. Naturally, these enzymes have extensively been exploited as therapeutic targets and considerable progress has been made.[2−8] Significant progress has been made toward the chemotherapy and prophylaxis of HIV infections.[9] A number of compounds have been licensed for clinical use, and additional compounds have proceeded through clinical and/or preclinical evaluation.[1,2,10−15] However, the continuing emergence of new HIV-1 variants resistant to the current treatments, together with cytotoxicity problems, makes the search for novel anti-HIV-1 drugs imperative.[3]

The mature HIV-1 envelope (Env) is composed of the outer membrane glycoprotein (gp) 120 and transmembrane gp41 subunits. The persistence of the infection by HIV-1 is believed to be related to the "wise" evolution of the structure of gp120 on the virion surface that can efficiently evade the immune system. Contributing elements include the heavy glycosylation on the surface,[16] residue variation,[17,18] oligomerization,[19,20] and conformational alterations.[21,22] HIV-1 entry into cells requires binding of the gp120 subunit of the viral Env glycoprotein to its primary receptor, CD4.[23,24] CD4 is a transmembrane glycoprotein expressed on the cell surface and is a member of the immunoglobulin (Ig) superfamily consisting of a large number of cell surface proteins with diverse biological functions.[25] The extracellular portion of CD4 consists of four Ig-like domains, D1−D4.[26−29] The gp120−CD4 binding induces a structural rearrangement in Env exposing conserved regions of the gp120 subunit, thereby enabling binding to an appropriate coreceptor, primarily the chemokine receptors CXCR4 or CCR5.[30,31] Further, engagement of gp120 to the coreceptor triggers conformational changes in the gp41 subunit, leading to the formation of a 6-helix coiled-coil (trimer-of-hairpins) that involves exposure and subsequent insertion of the gp41 fusion peptide into the target cell membrane. This facilitates fusion of virion envelope with the host cell membrane and release of the viral capsid into the cytosol.[32] Thus, these proteins have also become targets for anti-HIV-1 drug discovery and development, such as the ongoing development of CXCR4 antagonists, CCR5 antagonists, CD4 down-modulators, gp41-binding agents, and gp120-binding agents.[9]

The inhibition of HIV-1 entry as a therapeutic strategy has been recently validated by a clinical study demonstrating that a compound, T20, which targets gp41 and blocks HIV-1 entry, is highly efficient at controlling viral replication in patients.[33] This has raised the hope that HIV entry-blocking agents will be the next-generation anti-HIV drugs.[34]

The gp120 has been a major focus of AIDS research for more than a decade, as small molecules blocking the "socket" of gp120 with high affinity might prevent it from binding with CD4 and, therefore, block the initial step of the viral entry. We

* To whom correspondence should be addressed. E-mail: zhan@uky.edu. Telephone: 859-323-3943. Fax: 859-323-3575.

10.1021/jp0550762 CCC: $33.50
Published on Web 01/26/2006

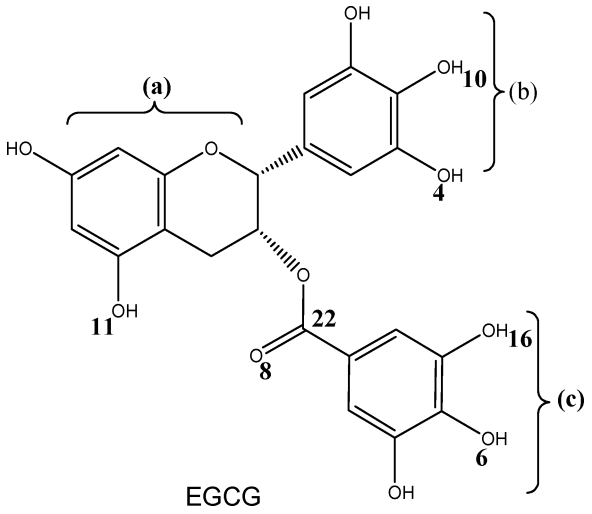

Figure 1. Molecular structure of catechin EGCG from green tea. Essential atoms implicated in the binding mode are numbered.

are particularly interested in blocking gp120−CD4 binding, because interaction between gp120 and CD4 is the initial step necessary for HIV-1 virus entry into the cells. When this initial step can be blocked, the virus will have no chance to enter into the cells. A possible inhibitor of gp120−CD4 binding can bind with either gp120 of the virus or CD4 of the cell in the conserved sites of gp120−CD4 binding.

Discovery and development of gp120−CD4 binding inhibitors have been objectives of research for a number of researchers, and some interesting gp120−CD4 binding inhibitors have been reported in the literature.[13,35−48] Different inhibitors may bind to the different protein sites, particularly different sites of CD4. Some interesting inhibitors were isolated from natural products. A remarkable compound is (−)-epigallocatechin gallate (EGCG) from green tea (Figure 1), which is currently the most potent inhibitor of gp120−CD4 binding. The anti-HIV-1 effect of EGCG was reported quite a few years ago,[49−52] although the detailed molecular mechanism was unknown. Recent experimental studies reported by Kawai et al.,[53] and highlighted by Nance and Shearer,[54] demonstrated that EGCG can effectively prevent CD4 binding with gp120, thus preventing the HIV-1 infection. Their data for EGCG interference with gp120 binding to CD4 protein suggests an IC_{50} value of ∼100 μM. Although an inhibitor with a significantly lower IC_{50} value is desirable for practical therapeutic use, EGCG provides a valuable template of such type of anti-HIV-1 entry inhibitors. More potent anti-HIV-1 entry inhibitors may be designed based on the mechanism concerning how EGCG can effectively prevent CD4 binding with gp120. Therefore, understanding how EGCG binds with CD4 and how EGCG can block gp120−CD4 binding should provide useful, fundamental insights into the mechanism for EGCG blocking CD4 binding with gp120 and into the future rational design of novel, next-generation anti-HIV-1 drugs.

Here we report some mechanistic insights obtained from extensive computational studies, including molecular docking, molecular dynamics (MD) simulations, and binding free energy calculations, on various possible three-dimensional (3D) structures of CD4−EGCG, gp120−CD4, and gp120−CD4−EGCG binding complexes based on high-performance supercomputing. The results reveal that EGCG binds with CD4 in such a mode that the affinity of gp120 binding with the CD4−EGCG complex is negligible. The simulated 3D binding structures and calculated binding free energies provide a rational basis for future design of novel, more potent inhibitors to block the gp120−CD4 binding.

Computational Methods

3D Model of the gp120−CD4 Complex. The initial coordinates of gp120−CD4 complex used in our computational studies came from the X-ray crystal structure (1RZJ) deposited in the Protein Data Bank.[55] The missing residues in the V3 (297−330) and V4 (397−410) loops of the X-ray crystal structure were built using a template structure, 1CE1,[56] and the automated homology modeling tool Modeler/InsightII software (Accelrys, Inc.).[57,58] Then, the best model was solvated in water and refined by performing a long MD simulation (see below for the MD procedure).

Molecular Docking. The first step of building the CD4−EGCG complex was to dock EGCG to CD4 by virtue of their geometric complementarity. We aimed to find where EGCG could be inserted most comfortably. Thus, the CD4 side chains were first relaxed by carrying out an MD simulation on CD4 in water (see below for the MD procedure) for 200 ps. Further, a visual inspection of the above-mentioned gp120−CD4 complex and an analysis of the solvent-accessible surface of the D1 domain of CD4 revealed a large and relatively deep surface cavity (pocket) plugged by V430 side chain of gp120. This pocket is constituted by the most important Phe43 and Arg59 residues of CD4 involved in the gp120−CD4 interaction. So, we first tested the possible binding of EGCG with this pocket (binding site) of CD4.

It is convenient to define a ligand-binding site model of CD4 receptor. The binding site was defined as a sphere centered on the Trp62 residue with an approximately 20-Å radius around the D1 domain of the CD4. The amino acid residues included in the binding site model were not contiguous in the protein. EGCG was initially positioned at ∼16 Å in front of Trp62 of the pocket. Docking calculations were performed on the EGCG compound with the CD4 binding site using the "automatic docking" Affinity module of the InsightII package (Accelrys, Inc.). The Affinity methodology[59] uses a combination of Monte Carlo type and simulated Annealing procedures to dock the guest molecule (the ligand) to the host (the receptor). A key feature is that the "bulk" of the receptor, defined as atoms not in the binding (active) site specified, is held rigid during the docking process, while the binding site atoms and ligand atoms are allowed to move. During the initial docking calculation process, a roughly docked CD4−EGCG complex was prepared. The Affinity module was used to energy-minimize starting structure. This process was designed to remove bad contacts and poor internal geometry in the initial structure and to obtain a reasonable starting point for subsequent search. The ligand was then moved by a random combination of translational, rotational, and torsional changes. The random movement of the ligand represents both the conformational space of the ligand and its orientation with respect to the receptor. This procedure has the advantage of overcoming any energy barrier on the potential energy surface. For each resulting randomly moved structures, the energy was evaluated and compared to that of the previously minimized structure. If the calculated energy change was within the specified (default) energy tolerance parameter, it was considered to have passed this first step and the structure was energy minimized. The second step was for fine tuning the docking. Whether the finally minimized structure was accepted or rejected was based on the Metropolis energy criterion as implemented in the software and its similarity to structures found before. The Metropolis criterion was found to be best suited

for finding a very small number of docked structures with very low energies (~100 lowest-energy structures were kept).

We have further refined these CD4−EGCG binding structures with the Simulated Annealing procedure (starting temperature at 400 K) and continued for 300-ps MD simulations at T = 298.15 K using the GB/SA implicit water model[60,61] to mimic the solvent environment. The energy minimization was performed by using the steepest descent algorithm first until the maximum energy derivative was smaller than 4 kcal/mol/Å and then using the conjugated gradient algorithm until the maximum energy derivative was smaller than 0.001 kcal mol^{-1} Å^{-1}. The MD simulation was performed with a time step of 1 fs. During the energy minimization and MD simulation, only ligand and side chains of amino acid residues of CD4 were allowed to move, while the backbone atoms of the protein were fixed. The energy minimizations and MD simulations for these processes were performed by using the Amber force field implemented in the Discover_3/InsightII calculation engine.[62] The nonbonded cutoff method and the dielectric constant were set up to group based (20-Å cutoff distance) and distance dependent ($\epsilon = 4r$), respectively.[63]

MD Simulation in Water. Each binding complex (or a free protein) simulated in this study was neutralized by adding an appropriate number of chloride counterions and was solvated in a rectangular box of TIP3P water molecules[64] with a minimum solute−wall distance of 10 Å. The partial atomic charges for the ligands were obtained after geometry optimization at the Hartree−Fock level with 6-31G* basis set and subsequent single-point calculation of the electrostatic potential, to which the charges were fitted using the RESP procedure.[65,66] Force-field parameters of the ligands were assigned based on the atom types of the force field model developed by Cornell et al.[62] Gaussian 03[67] was used to optimize the molecular structure and generate electrostatic potentials.

The MD simulations were performed by using the Sander module of the Amber7 program,[68] in the way similar to what we did for other protein−ligand systems.[69] The solvated system was optimized prior to the MD simulation. First of all, the simulated binding complex was frozen and the solvent water molecules and counterions were allowed to move during a 5000-step minimization with the conjugate gradient algorithm and a 5 ps MD run at T = 298.15 K. After the full relaxation and the entire solvated system was energy minimized, the system was slowly heated from T = 10 to 298.15 K in 70 ps before a sufficiently long MD simulation in room temperature. The MD simulations were performed with a periodic boundary condition in the NPT ensemble at T = 298.15 K with Berendsen temperature coupling[70] and constant pressure (P = 1 atm) with isotropic molecule-based scaling.[70] The SHAKE algorithm[71] was applied to fix all covalent bonds containing a hydrogen atom, a time step of 2 fs was used, and the nonbond pair list was updated every 10 steps. The pressure was adjusted by isotropic position scaling. The particle mesh Ewald (PME) method[72] was used to treat long-range electrostatic interactions. A residue-based cutoff of 10 Å was applied to the noncovalent interactions. During the MD simulation, the coordinates of the simulated complex were saved every 1 ps.

Binding Free-Energy Calculation. The binding free energies were calculated by using the molecular mechanics−Poisson−Boltzmann surface area (MM-PBSA) free-energy calculation method.[73] In the MM-PBSA method, the free energy of the inhibitor binding, ΔG_{bind}, is obtained from the difference between the free energies of the receptor−ligand complex (G_{cpx}) and the unbound receptor (G_{rec}) and ligand (G_{lig}) as following

$$\Delta G_{bind} = G_{cpx} - (G_{rec} + G_{lig}) \quad (1)$$

The averaged structure was obtained from the last 200 selected "snapshot" structures taken from the MD trajectory of the studied system. The final structure was then energy-minimized in implicit water by using a GB/SA continuum solvation model.[74,75] The geometry refinement was carried out using the Sander module of Amber7 program[68] via a combined steepest descent/conjugate gradient algorithm, using a convergence criterion of 0.01 kcal mol^{-1} Å^{-1} for the maximum energy gradient.

The binding free energy (ΔG_{bind}) was evaluated as a sum of the changes in the MM gas-phase binding energy (ΔE_{MM}), solvation free energy (ΔG_{solv}), and entropy contribution ($-T\Delta S$)- The MM binding energies were calculated with the Sander

$$\Delta G_{bind} = \Delta E_{bind} - T\Delta S \quad (2)$$

$$\Delta E_{bind} = \Delta E_{MM} + \Delta G_{solv} \quad (3)$$

$$\Delta E_{MM} = \Delta E_{ele} + \Delta E_{vdw} \quad (4)$$

$$\Delta G_{solv} = \Delta G_{PB} + \Delta G_{np} \quad (5)$$

$$\Delta G_{np} = \gamma \mathrm{SASA} + \beta \quad (6)$$

module of Amber7 program.[68] Electrostatic solvation free energy was calculated by the finite-difference solution to the PB equation (ΔG_{PB}) as implemented in the Delphi program.[76,77] The dielectric constants used are 1 for the solute and 80 for the solvent water. The MSMS program[78] was used to calculate the SASA for the estimation of the nonpolar solvation energy (ΔG_{np}) using eq 6 with the default parameters, i.e., γ = 0.00542 kcal/Å^2 and β = 0.92 kcal/mol. Further, the entropy contribution, $-T\Delta S$, to the binding free energy was also calculated for the CD4−EGCG complex at T = 298.15 K by using the nmode module of Amber7 program, which is based on a combination of the standard classical statistical formulas[79] and normal-mode analysis.[80] In addition, we also carefully made the necessary energy correction due to the standard reference state change from the gas-phase density associated with P = 1 atm to the solution concentration at 1 M to the $-T\Delta S$ value, as we did in other first-principles solvation studies.[81]

Most of the MD simulations in water were performed on a HP supercomputer, Superdome, at the Center for Computational Sciences, University of Kentucky. The other computations were carried out on SGI Fuel workstations and a 34-processors IBM ×335 Linux cluster in our own lab.

Results and Discussion

EGCG Binding with CD4. The molecular docking and MD simulations were performed to reveal how CD4 binds with EGCG and to predict the corresponding CD4−EGCG binding free energy. The ligand-binding pocket of CD4 consists of Phe43 and Arg59 residues implicated in the gp120−CD4 interaction. In the most favorable one of the CD4−EGCG binding modes found in the present study, the gallate moiety of EGCG was close to the side chains of Arg59 and Phe43 residues. The simulated average distances between the carbonyl carbon C22 of the gallate ester of EGCG and Cα atoms of Phe43 and Arg59 were 7.8 and 6.0 Å, respectively. Two H bonds existed between CD4 and hydroxyl groups of EGCG. These two H bonds involve the NH2 group of Asn39 side chain and the NH backbone of Ile24. The finally simulated CD−EGCG binding structure is depicted in Figure 2. As shown in Figure 2, EGCG is also

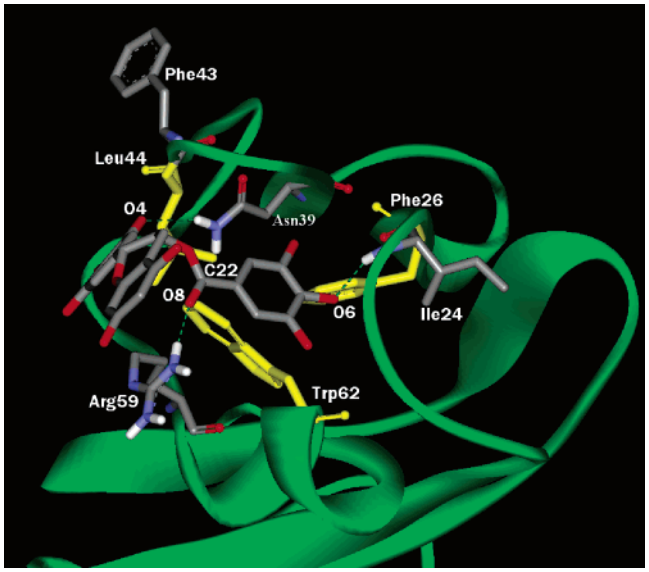

Figure 2. EGCG binding with the D1 domain of CD4 binding site in the simulated CD4−EGCG binding complex. Only amino acid residues close to EGCG are displayed for clarity.

stabilized in the cavity of CD4 by an edge-to-face $\pi-\pi$ interaction between the indole group of Trp62 and the two phenyl rings of EGCG. There is also a $\pi-\pi$ stacking interaction between the guanidinium group of Arg59 side chain and the dihydro−chromene group of EGCG.

In the calculation of the CD4−EGCG binding free energy (ΔG_{bind}), we obtained $\Delta E_{bind} = -20.4$ kcal/mol, and $-T\Delta S = 14.9$ kcal/mol (including the energy correction of the standard reference state) at $T = 298.15$ K. Thus, we have $\Delta G_{bind} = -5.5$ kcal/mol for the CD4−EGCG binding, as seen in Table 1. On the basis of the calculated ΔG_{bind} value of −5.5 kcal/mol, the dissociation constant (K_d) of the CD4−EGCG complex is estimated to be 9.4×10^{-5} M (or 94 μM), which is very close to the experimental data,[53] suggesting an IC_{50} value of ∼100 μM for EGCG blocking CD4−gp120 binding.

Glycoprotein gp120 Binding with CD4. Available experimental data indicate that the CD4 antigen on the cell surface interacts with the gp120 of the virus via a depression in the gp120 molecule that lacks carbohydrate chains.[82,83] The direct contacts between the two proteins involve 22 CD4 amino acids and 26 gp120 amino acids, but the residues that are most important in this association are Trp427, Glu370, Gly473, and Ile371 of gp120 interacting with Phe43 of CD4 and Val430 of gp120 interacting with Arg59 of CD4.[82,83] The importance of these residues was highlighted by site-directed mutagenesis studies in which the mutations on Asp368, Glu370, and Trp427 of gp120 diminished the affinity of CD4 to the gp120 mutants.[83] In addition, a survey of the gp120−CD4 binding interface close to Phe43 of CD4 reveals a strong electrostatic interaction between Asp368 of gp120 and Arg59 of CD4.

It should be pointed out that the best gp120−CD4 binding mode found in the X-ray crystal structure is not necessarily the best gp120−CD4 binding mode in solution. So, we decided to perform a sufficiently long MD simulation on this particularly interesting protein−protein interaction in water and attempted to obtain a stable MD trajectory in order to reliably calculate the gp120−CD4 binding free energy. For this purpose, the missing residues of V3 and V4 loops were added to the gp120 model by homology modeling before performing a long MD simulation for 6.5 ns. Figure 3 reveals that the MD trajectory of the simulated gp120−CD4 complex became stable after ∼2.8 ns with a root-mean-square deviation (RMSD) of 2.9 Å from the starting structure. The stability of the gp120−CD4 binding mode is described by some internuclear distances between some key amino acid residues. The protein−protein interaction in the simulated gp120−CD4 complex is essentially the same as that in the X-ray crystal structure. It is notable that the hydrogen bonds between Asp368 of gp120 and Arg59 of CD4 are well conserved and that Phe43 of CD4 is also well stabilized in the pocket formed by Trp427 and Asp368 of gp120.

On the basis of the stable MD trajectory for the gp120−CD4 binding, the ΔE_{bind} value for the gp120−CD4 binding was calculated to be −44.1 kcal/mol, as seen in Table 1. We were unable to directly calculate the $-T\Delta S$ value for this protein−protein complex, which is too large to perform a normal-mode analysis even with the supercomputer (with a very large shared memory) available to us. Nevertheless, available thermodynamic experimental data can be utilized to estimate the $-T\Delta S$ value for gp120−CD4 binding. As seen in Table 1, for the gp120−CD4 binding, thermodynamic experimental data reported by different labs are considerably different in terms of the separate ΔH (or ΔE_{bind}) and $-T\Delta S$ values.[84,85] Nevertheless, the final binding free energy (ΔG_{bind}) values (−10.2 ± 0.1 and −9.5 ± 0.1 kcal/mol) are very close to each other. Our calculated ΔE_{bind} value of −44.1 kcal/mol is close to the lower one of the two available experimental ΔE_{bind} values (−48.4 ± 2.5 and −62 ± 3 kcal/mol).[84,85] Further, we may take the average experimental ΔG_{bind} value, about −9.9 kcal/mol, as a standard reference and use our calculated ΔE_{bind} value of −44.1 kcal/mol to estimate the $-T\Delta S$ value. Thus we have $-T\Delta S = 34.2$ kcal/ mol. The estimated $-T\Delta S$ value of 34.2 kcal/mol will be used, along with the calculated ΔE_{bind} values, to evaluate the free energy of gp120 binding with the CD4−EGCG complex.

Glycoprotein gp120 Binding with CD4−EGCG Complex. The final CD4−EGCG binding structure obtained from the MD simulation was superimposed with the simulated gp120−CD4 complex in order to build the initial structure of the gp120−CD4−EGCG complex for carrying out the MD simulation on such a protein−protein−ligand binding complex in water. After the superimposing and replacement, the gp120 protein in the complex was slightly moved away from its initial location to avoid bad contacts between the ligand and the protein side chains. The MD simulation starting from this carefully built initial structure eventually led to a stable MD trajectory.

Figure 4 demonstrates the MD-simulated most important internuclear distances and hydrogen bonds between EGCG and the proteins. The CD4−EGCG interaction in the simulated gp120−CD4−EGCG complex was essentially the same as that in the simulated CD4−EGCG complex. However, the gp120−CD4 interaction in the simulated gp120−CD4−EGCG complex was significantly different from that in the simulated gp120−CD4 complex. This is because the existence of ligand EGCG prevents formation of some important interaction between gp120 and CD4. The hydrogen bond between the Arg59 of CD4 and the O8 carboxyl group of EGCG was persistent during the MD simulation, with an average dynamic length equal to ∼1.9 Å. EGCG was stabilized by two other hydrogen bonds with the NH backbone of Gly431 of gp120 and the amine group of Asn39 side chain of CD4. Figure 5 shows the simulated structure of the gp120−CD4−EGCG complex, in which the dihydrochromene ring and gallate group of EGCG fill the entire binding site cavity consisting of amino acid residues 37−47 and 56−59 of CD4. Further, the ester group of EGCG is in an orientation favorable for its interaction with Arg59 and Asn39 side chains of CD4. Figure 6 shows the superposition of the MD-simulated

TABLE 1: Calculated and Experimental Energetic Data (kcal/mol) at T = 298.15 K

	CD4−EGCG		gp120−CD4		gp120−(CD4−EGCG)
	calcd	exptl	exptl[b]	calcd	calcd
ΔE^{ele}_{int}	−29.3			−2.0	−87.1
ΔE^{vdw}_{int}	−43.1			−123.7	−145.1
ΔE_{MM}	−72.4			−125.7	−232.2
ΔG_{sol}	52.1			81.6	195.2
ΔG^{ele}_{tot}	25.8			86.3	115.8
ΔE_{bind} [or ΔH]	−20.4		−48.4 ± 2.5 (−62 ± 3)	−44.1	−37.1
$-T\Delta S$	14.9		38.2 ± 2.5 (52.5 ± 3)	34.2[c]	
ΔG_{bind}	−5.5	∼−5.4[a]	−10.2 ± 0.1 (−9.5 ± 0.1)	−9.9	−2.9[d]

[a] The experimental value was roughly estimated from the experimental data in ref 53 that suggests an IC_{50} value of ∼100 μM for EGCG blocking CD4−gp120 binding. [b] The experimental data is from ref 84. The values in parentheses came from ref 85. [c] The entropy contribution was estimated by using the calculated ΔE_{bind} value of −44.1 kcal/mol and the average value (−9.9 kcal/mol) of the experimental ΔG_{bind} values for the gp120−CD4 binding. [d] The result based on the assumption that the entropy contribution to the gp120−CD4 binding free energy in the simulated gp120−CD4−EGCG complex is the same as that of 34.2 kcal/mol in the gp120−CD4 complex.

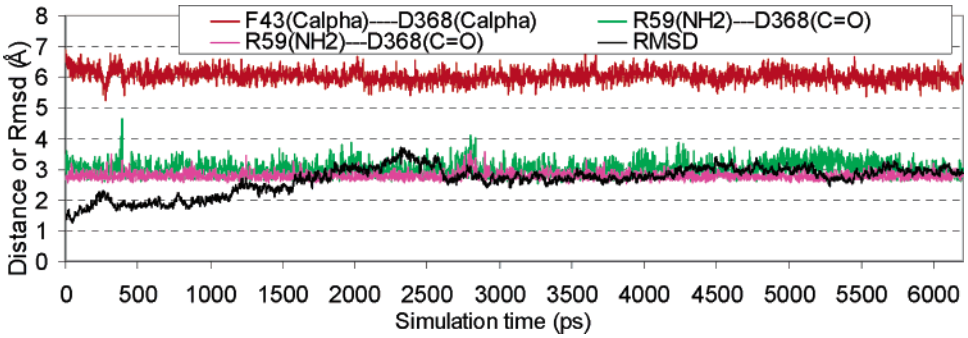

Figure 3. Plots of the key internuclear distances in the simulated gp120−CD4 complex vs the simulation time. RMSD (in Å) of the simulated positions of the complex Cα trace atoms from those in the starting structure is also shown.

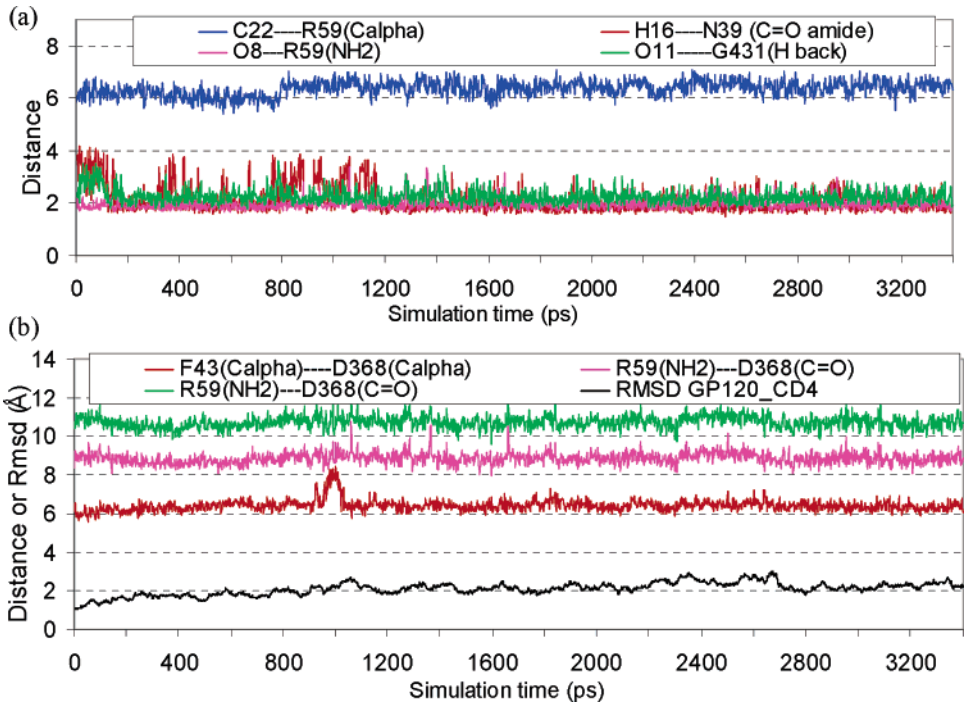

Figure 4. Both (a) and (b) are plots of the key internuclear distances in the simulated gp120−CD4−EGCG complex vs the simulation time. RMSD in (b) represents the root-mean-square deviation (in Å) of the simulated positions of the Cα trace atoms of gp120−CD4 from those in the starting structure.

final structure of the gp120−CD4−EGCG complex with that of the gp120−CD4 complex. Two major conformational changes were observed in the binding pocket. The hydrogen bonding interaction between Arg59 of CD4 and Asp368 of gp120 was disrupted by EGCG. The particular conformation of EGCG in the binding site of CD4 prevents the Val430 of gp120 to fill the hydrophobic pocket of CD4.

As observed in the aforementioned MD simulation on the CD4−EGCG complex, the MD simulation on the gp120−CD4−EGCG complex also revealed that EGCG was stabilized in the binding site by forming a strong π-stacking interaction with the guanidinium group of Arg59 side chain of CD4 and a cation−π interaction with the ϵ-amine group of Lys432 side chain in gp120. The plane formed by the pyrogallol ring was

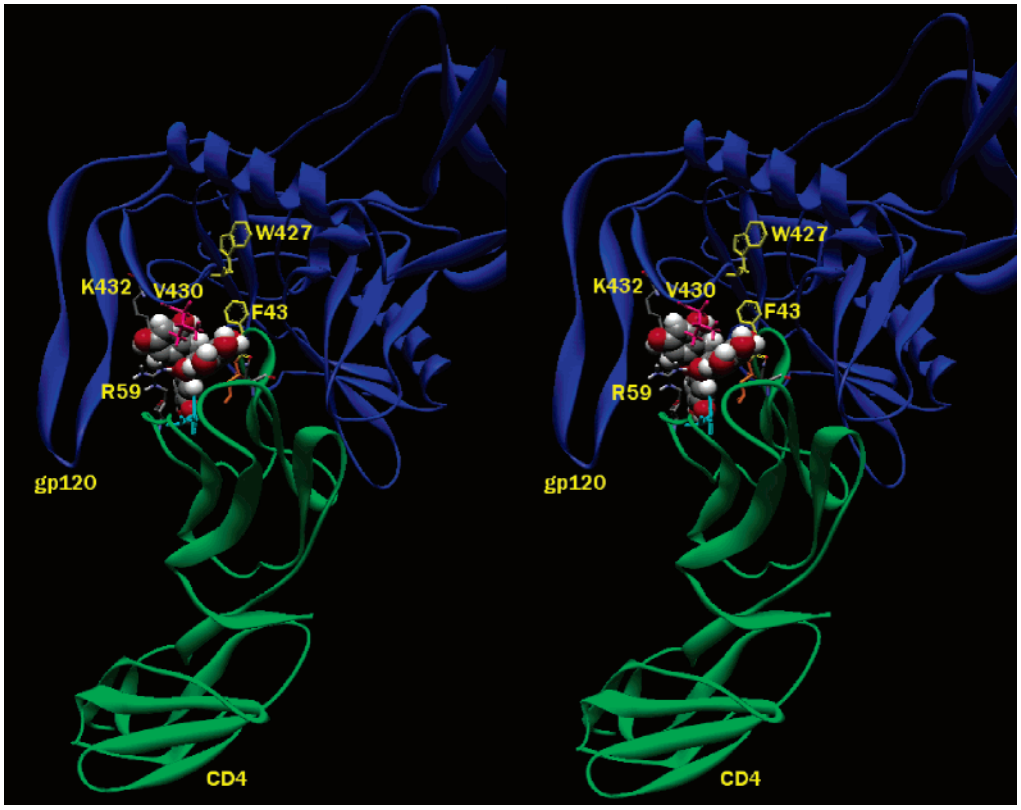

Figure 5. Stereoview of EGCG binding with gp120 and CD4 in the simulated gp120−CD4−EGCG complex. Only amino acid residues close to EGCG are displayed for clarity.

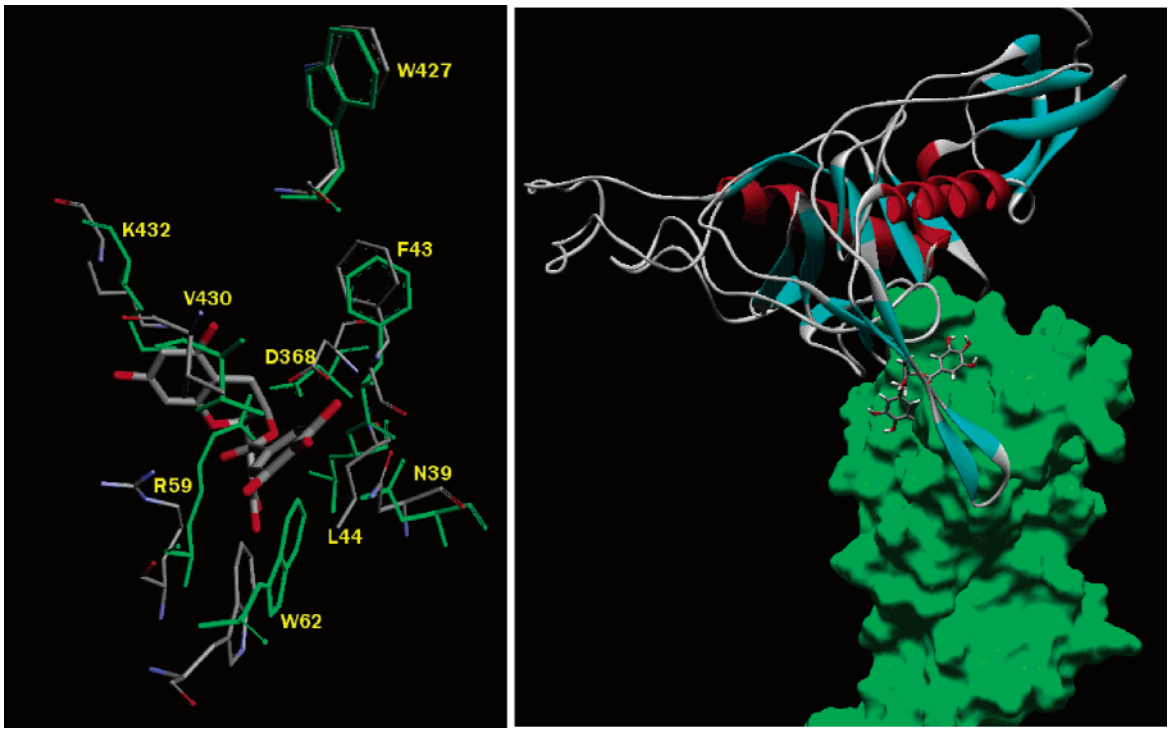

Figure 6. Left side: Superposition of the MD-simulated final structure of the gp120−CD4−EGCG complex with that of the gp120−CD4 complex (green), showing the disruption of the hydrogen bonding between $gp120^{D368}$ with $CD4^{R59}$ residues in the gp120−CD4−EGCG complex. Only essential residues of CD4 and gp120 surrounding EGCG are shown. Right side: Binding mode of EGCG in the gp120−CD4 complex.

quasiparallel to the plane formed by the guanidinium group of Arg59 side chain in CD4, with a short distance of about 3.5 Å. In addition, the aromatic rings of EGCG were also stabilized in the binding site cavity by the dipole−quadrupole interactions between the Val430 side chain of gp120 and the dihydrochromene ring and gallate group of EGCG and between the Leu44 side chain of CD4 and the pyrogallol ring of EGCG.

As seen in Table 1, the calculated ΔG_{bind} value (−2.9 kcal/mol) of the gp120−CD4 binding in the simulated gp120−CD4−EGCG complex is considerably different from the corresponding

ΔG_{bind} value (−9.9 kcal/mol) of the gp120−CD4 binding in the simulated gp120−CD4 complex. The binding affinity of CD4 with gp120 is considerably reduced after EGCG binds to CD4. This shows that EGCG can effectively prevent CD4 binding with gp120, which is consistent with the aforementioned experimental observation.

Conclusion

Molecular docking, MD simulations, and binding free-energy calculations have demonstrated the most favorable structures of binding among the solvated glycoprotein gp120 of the HIV-1 virus, glycoprotein CD4 of the cell, and EGCG from green tea. Stable MD trajectories have been obtained for the simulated CD4−EGCG, gp120−CD4, and gp120−CD4−EGCG binding complexes in water. In both the favorable CD4−EGCG and gp120−CD4−EGCG complexes simulated, EGCG was stabilized right in the gp120 binding site of CD4 such that CD4 could not effectively bind with gp120. The calculated binding free energies (ΔG_{bind}) are −5.5 kcal/mol for EGCG binding with CD4, −9.9 kcal/mol for gp120 binding with CD4, and −2.9 kcal/mol for gp120 binding with the CD4−EGCG complex. So, the binding of EGCG with CD4 can effectively block CD4 binding with gp120 of HIV-1 virus. The calculated results are consistent with the experimental observation that EGCG can effectively prevent the HIV-1 infection through blocking gp120−CD4 binding. On the basis of the calculated CD4−EGCG binding free energy (ΔG_{bind}) of −5.5 kcal/mol, the predicted dissociation constant (K_d) of 94 μM is in excellent agreement with the experimental data suggesting an IC_{50} value of ∼100 μM for EGCG blocking CD4 binding with gp120. These fundamental insights into the binding structures and inhibitory mechanism of EGCG provide a rational basis for future design of novel, more potent inhibitors to block the gp120−CD4 binding.

Acknowledgment. The research was supported in part by NIH/NIDA (Grant R01DA013930 to C.-G. Zhan) and by the College of Pharmacy and Center for Computational Sciences (CCS) at University of Kentucky. The authors also acknowledge the CCS for supercomputing time on Superdome.

References and Notes

(1) De Clercq, E. in *Combination Therapy of AIDS*; De Clercq, E., Vandamme, A.-M., Eds.; Birkhauser Verlag: Basel, Switzerland, 2004; pp 1−24.
(2) http://www.aidsmeds.com.
(3) http://www. WHO.org.
(4) Culshaw, R. V. *J. Biol. Systems* **2004**, *12*, 123.
(5) Berkhout, B. *Curr. Opin. Mol. Ther.* **2004**, *6*, 141.
(6) Ast, O.; Luke, W. *Curr. Opin. Mol. Ther.* **2004**, *6*, 302.
(7) Locatelli, G. A.; Cancio, R.; Spadari, S.; Maga, G. *Curr. Drug Metab.* **2004**, *5*, 283.
(8) Witvrouw, M.; Van Maele, B.; Vercammen, J.; Hantson, A.; Engelborghs, Y.; De Clercq, E.; Pannecouque, C.; Debyser, Z. *Curr. Drug Metab.* **2004**, *5*, 291.
(9) De Clercq, E. *Int. J. Biochem. Cell. B.* **2004**, *36*, 1800.
(10) Ena, J.; Pasquau, F. *Clin. Infect. Dis.* **2003**, *36*, 1186.
(11) Louie, M.; Hogan, C.; Hurley, A.; Simon, V.; Chung, C.; Padte, N.; Lamy, P.; Flaherty, J.; Coakley, D.; Di Mascio, M.; Perelson, A. S.; Markowitz, M. *AIDS* **2003**, *17*, 1151.
(12) Louie, M.; Hogan, C.; Di Mascio, M.; Hurley, A.; Simon, V.; Rooney, J.; Ruiz, N.; Brun, S.; Sun, E.; Perelson, A. S.; Ho, D. D.; Markowitz, M. *J. Infect. Dis.* **2003**, *187*, 896.
(13) Pierson, T. C.; Doms, R. W.; Pohlmann, S. *Rev. Med. Virol.* **2004**, *14*, 255.
(14) Deval, J.; Courcambeck, J.; Selmi, B.; Boretto, J.; Canard, B. *Curr. Drug Metab.* **2004**, *5*, 305.
(15) Enanoria, W. T. A.; Ng, C.; Saha, S. R.; Colford, J. M. *Lancet Infect. Dis.* **2004**, *4*, 414.
(16) Leonard, C. K.; Spellman, M. W.; Riddle, L.; Harris, R. J.; Thomas, J. N.; Gregory, T. J. *J. Biol. Chem.* **1990**, *265*, 10373.
(17) Wei, X.; Decker, J. M.; Wang, S.; Hui, H.; Kappes, J. C.; Wu, X.; Salazar-Gonzalez, J. F.; Salazar, M. G.; Kilby, J. M.; Saag, M. S.; Komarova, N. L.; Nowak, M. A.; Hahn, B. H.; Kwong, P. D.; Shaw, G. M. *Nature* **2003**, *422*, 307 and **2004**, *423*, 197.
(18) Arendrup, M.; Nielsen, C.; Hansen, J. E.; Pedersen, C.; Mathiesen, L.; Nielsen, J. O. *AIDS* **1992**, *5*, 303.
(19) Weiss, C. D.; Levy, J. A.; White, J. M. *J. Virol.* **1990**, *64*, 5674.
(20) Kwong, P. D.; Wyatt, R.; Sattentau, Q. J.; Sodroski, J.; Hendrickson, W. A. *J. Virol.* **2000**, *74*, 1961.
(21) (a) Kwong, P. D.; Wyatt, R.; Robinson, J.; Sweet, R. W.; Sodroski, J.; Hendrickson, W. A. *Nature* **1998**, *393*, 648. (b) Kwong, P. D.; Doyle, M. L.; Casper. D. J.; Cicala, C.; Leavitt, S. A.; Majeed. S.; Steenbeke, T. D.; Venturi, M.; Chaiken, I.; Fung, M.; Katinger, H.; Parren, P. W. L. H.; Robinson. J.; Van Ryk. D.; Wang, L. P.; Burton, D. R.; Freire, E.; Wyatt, R.; Sodroski, J.; Hendrickson, W. A.; Arthos, J. *Nature* **2002**, *420*, 678.
(22) (a) Xiang, S. H.; Kwong, P. D.; Gupta, R.; Rizzuto, C. D.; Casper, D. J.; Wyatt, R.; Wang, L.; Hendrickson, W. A.; Doyle, M. L.; Sodroski, J. *J. Virol.* **2002**, *76*, 9888. (b) Xiang, S. H.; Wang, L. P.; Abreu, M.; Huang, C. C.; Kwong, P. D.; Rosenberg, E.; Robinson, J. E.; Sodroski, J. *Virol.* **2003**, *315*, 124.
(23) (a) Dalgleish, A. G.; Beverley, P. C.; Clapham, P. R.; Crawford, D. H.; Greaves, M. F.; Weiss, R. A. *Nature* **1984**, *312*, 763. (b) Sattentau, Q. J.; Dalgleish, A. G.; Weiss, R. A.; Beverley, P. C. L. *Science* **1986**, *234*, 1120.
(24) Klatzmann, D.; Champagne, E.; Chamaret, S.; Gruest, J.; Guetard, D.; Hercend, T.; Gluckman, J. C.; Montagnier, L. *Nature* **1984**, *312*, 767.
(25) Parnes, J. R. *Adv. Immunol.* **1989**, *44*, 256.
(26) Brady, R. L.; Dodson, E. J.; Dodson, G. G.; Lange, G.; Davis, S. J.; Williams, A. F.; Barclay, A. N. *Science* **1993**, *260*, 979.
(27) Harris, R. J.; Chamow, S. M.; Gregory, T. J.; Spellman, M. W. *Eur. J. Biochem.* **1990**, *188*, 291.
(28) Ryu, S. E.; Kwong, P. D.; Truneh, A.; Porter, T. G.; Arthos, J.; Rosenberg, M.; Dai, X. P.; Xuong, N. H.; Axel, R.; Sweet, R. W.; Hendrickson, W. A. *Nature* **1990**, *348*, 419.
(29) Wang, J. H.; Yan, Y. W.; Garrett, T. P.; Liu, J. H.; Rodgers, D. W.; Garlick, R. L.; Tarr, G. E.; Husain, Y.; Reinherz, E. L.; Harrison, S. C. *Nature* **1990**, *348*, 411.
(30) Berger, E. A.; Murphy, P. M.; Farber, J. M. *Annu. Rev. Immunol.* **1999**, *17*, 657.
(31) Doms, R. W.; Moore, J. P. *J. Cell Biol.* **2000**, *151*, F9.
(32) Eckert, D. M.; Kim, P. S. *Annu. Rev. Biochem.* **2001**, *70*, 777.
(33) Kilby J. M.; Hopkins S.; Venetta T. M.; Di-Massimo B.; Cloud G. A.; Lee J. Y.; Alldredge L.; Hunter E.; Lambert D.; Bolognesi D.; Matthews T.; Johnson M. R.; Nowak M. A.; Shaw G. M.; Saag M. S. *Nat. Med.* **1998**, *4*, 1302.
(34) Blair, W. S.; Lin, P. F.; Meanwell, N. A.; Wallace, O. B. *Drug Discov. Today* **2000,** *5*, 183.
(35) Huang, Z.; Li, S.; Korngold, R. *Biopolymers* **1997**, *43*, 367.
(36) Edling, A. E.; Choksi, S.; Huang, Z. W.; Korngold, R. *J. Autoimmun.* **2002**, *18*, 169.
(37) Prakash, K.; Zhao, L.; Fisch, D.; Rosenfield, S.; Nagashima, K.; Schulke, N.; Olson, W. *Abst. Papers Am. Chem. Soc.* **2003**, *225*, U231−U232 295-BIOT Part 1.
(38) Este, J. A. *Curr. Med. Chem.* **2003**, *10*, 1617.
(39) Zaitseva, M.; Peden, K.; Golding, H. *Biochim. Biophys. Acta* **2003**, *1614*, 51.
(40) Jiang, X. H.; Song, Y. L.; Long, Y. Q. *Bioorg. Med. Chem. Lett.* **2004**, *14*, 3675.
(41) Kuhmann, S. E.; Moore, J. P. *Trends Pharmacol. Sci.* **2004**, *25*, 117.
(42) Li, H. G.; Song, H. J.; Heredia, A.; Le, N.; Redfield, R.; Lewis, G. K.; Wang, L. X. *Bioconj. Chem.* **2004**, *15*, 783.
(43) De Clercq, E. *Int. J. Biochem. Cell B.* **2004**, *36*, 1800.
(44) Seibert, C.; Sakmar, T. P. *Curr. Pharm. Design* **2004**, *10*, 2041.
(45) Wang, H. G. H.; Williams, R. E.; Lin, P. F. *Curr. Pharm. Design* **2004**, *10*, 1785.
(46) Liu, S. W.; Jiang. S. B. *Curr. Pharm. Design* **2004**, *10*, 1827.
(47) Yuan, W.; Craig, S.; Si, Z. H.; Farzan, M.; Sodroski, J. *J. Virol.* **2004**, *78*, 5448.
(48) Tomkowicz, B.; Collman, R. G. *Expert Opin. Ther. Targets* **2004**, *8*, 65.
(49) Nakane, H.; Ono, K. *Nucleic Acids Symp. Ser.* **1989**, *21*, 115.
(50) Harada, S.; Haneda, E.; Maekawa, T.; Morikawa, Y.; Funayama, S.; Nagata, N.; Ohtsuki, K.; Nagata, N.; Ohtsuki, K. *Biol. Pharm. Bull.* **1999**, *22*, 1122.
(51) Yamaguchi, K.; Honda, M.; Ikigai, H.; Hara, Y.; Shimamura, T. *Antiviral Res.* **2002**, *53*, 19.
(52) Fassina, G.; Buffa, A.; Benelli, R.; Varnier, O. E.; Noonan, D. M.; Albini, A. *AIDS* **2002**, *6*, 939.

(53) Kawai, K.; Tsuno, N. H.; Kitayama, J.; Okaji, Y.; Yazawa, K.; Asakage, M.; Hori, N.; Watanabe, T.; Takahashi, K.; Nagawa, H. *J. Allergy Clin. Immun.* **2003**, *112*, 951.

(54) Nance, C. L.; Shearer, W. T. *J. Allergy Clin. Immun.* **2003**, *112*, 851.

(55) (a) Bernstein, F. C.; Koetzle, T. F.; Williams, G. J.; Meyer, E. E., Jr.; Brice, M. D.; Rodgers, J. R.; Kennard, O.; Shimanouchi, T.; Tasumi, M. *J. Mol. Biol*. **1977**, *112*, 535. (b) http://www.rcsb.org/pdb/.

(56) James, L. C.; Hale, G.; Waldmann, H.; Bloomer, A. C. *J. Mol. Biol*. **1999**, *289*, 293.

(57) Sali, A.; Blundell, T. L. *J. Mol. Biol*. **1990**, *212*, 403.

(58) Sali, A.; Blundell, T. L. *J. Mol. Biol*. **1993**, *234*, 779.

(59) Kuntz, I. D.; Meng, E. C.; Shoichet, B. K. *Acc. Chem. Res* **1994**, *27*, 117.

(60) Still, W. C.; Tempczyk, A.; Hawley, R. C.; Hendrickson, T. *J. Am. Chem. Soc.* **1990**, *112*, 6127.

(61) Weiser, J.; Shenkin, P. S.; Still, W. C. *J. Comput. Chem*. **1999**, *20*, 217.

(62) Cornell, W. D.; Cieplak, P.; Bayly, C. I.; Gould, I. R.; Merz, K. M., Jr.; Ferguson, D. M.; Spellmeyer, D. C.; Fox, T.; Caldwell, J. W.; Kollman, P. A. *J. Am. Chem. Soc.* **1995**, *117*, 5179.

(63) Harvey, S. C. *Proteins* **1989**, *5*, 78.

(64) Jorgensen, W. L.; Chandrasekhar, J.; Madura, J. D.; Impey, R. W.; Klein, M. L. *J. Chem. Phys*. **1983**, *79*, 926.

(65) Bayly, C. I.; Cieplak, P.; Cornell, W. D.; Kollman, P. A. *J. Phys. Chem.* **1993**, *97*, 10269.

(66) Cornell, W. D.; Cieplak, P.; Bayly, C. I.; Kollman, P. A. *J. Am. Chem. Soc*. **1993**, *115*, 9620.

(67) Frisch, M. J.; Trucks, G. W.; Schlegel, H. B.; Scuseria, G. E.; Robb, M. A.; Cheeseman, J. R.; Montgomery, J. A., Jr.; Vreven, T.; Kudin, K. N.; Burant, J. C.; Millam, J. M.; Iyengar, S. S.; Tomasi, J.; Barone, V.; Mennucci, B.; Cossi, M.; Scalmani, G.; Rega, N.; Petersson, G. A.; Nakatsuji, H.; Hada, M.; Ehara, M.; Toyota, K.; Fukuda, R.; Hasegawa, J.; Ishida, M.; Nakajima, T.; Honda, Y.; Kitao, O.; Nakai, H.; Klene, M.; Li, X.; Knox, J. E.; Hratchian, H. P.; Cross, J. B.; Adamo, C.; Jaramillo, J.; Gomperts, R.; Stratmann, R. E.; Yazyev, O.; Austin, A. J.; Cammi, R.; Pomelli, C.; Ochterski, J. W.; Ayala, P. Y.; Morokuma, K.; Voth, G. A.; Salvador, P.; Dannenberg, J. J.; Zakrzewski, V. G.; Dapprich, S.; Daniels, A. D.; Strain, M. C.; Farkas, O.; Malick, D. K.; Rabuck, A. D.; Raghavachari, K.; Foresman, J. B.; Ortiz, J. V.; Cui, Q.; Baboul, A. G.; Clifford, S.; Cioslowski, J.; Stefanov, B. B.; Liu, G.; Liashenko, A.; Piskorz, P.; Komaromi, I.; Martin, R. L.; Fox, D. J.; Keith, T.; Al-Laham, M. A.; Peng, C. Y.; Nanayakkara, A.; Challacombe, M.; Gill, P. M. W.; Johnson, B.; Chen, W.; Wong, M. W.; Gonzalez, C.; Pople, J. A. *Gaussian 03*, revision A.1; Gaussian, Inc.: Pittsburgh, PA, 2003.

(68) Case, D. A.; Pearlman, D. A.; Caldwell, J. W.; Cheatham, T. E., III; Wang, J.; Ross, W. S.; Simmerling, C. L.; Darden, T. A.; Merz, K. M.; Stanton, R. V.; Cheng, A. L.; Vincent, J. J.; Crowley, M.; Tsui, V.; Gohlke, H.; Radmer, R. J.; Duan, Y.; Pitera, J.; Massova, I.; Seibel, G. L.; Singh, U. C.; Weiner, P. K.; Kollman, P. A. *AMBER 7*; University of California, San Francisco, 2002.

(69) (a) Zhan, C.-G.; Norberto de Souza, O.; Rittenhouse, R.; Ornstein, R. L. *J. Am. Chem. Soc.* **1999**, *121*, 7279. (b) Koca, J.; Zhan, C.-G.; Rittenhouse, R.; Ornstein, R. L. *J. Am. Chem. Soc*. **2001**, *123*, 817. (c) Koca**,** J.; Zhan, C.-G.; Rittenhouse, R. C.; Ornstein, R. L. *J. Comput. Chem.* **2003**, *24*, 368. (d) Zhan, C.-G.; Zheng, F.; Landry, D. W. *J. Am. Chem. Soc.* **2003**, *125*, 2462. (e) Hamza, A.; Cho, H.; Tai, H.-H.; Zhan, C.-G. *J. Phys. Chem. B* **2005**, *109*, 4776. (f) Hamza, A.; Cho, H.; Tai, H.-H.; Zhan, C.-G. *Bioorg. Med. Chem.* **2005**, *13*, 4544. (g) Pan, Y.; Gao, D.; Yang, W.; Cho, H.; Yang, G.-F.; Tai, H.-H.; Zhan, C.-G. *Proc. Natl. Acad. Sci. U.S.A.* **2005**, *102*, 16656. (h) Gao, D.; Zhan, C.-G. *J. Phys. Chem. B* **2005** *109*, 23070. (i) Gao, D.; Zhan, C.-G. *Proteins* **2006**, *62*, 99.

(70) Berendsen, H. J. C.; Postma, J. P. M.; van Gunsteren, W. F.; DiNola, A.; Haak, J. R. *J. Chem. Phys*. **1984**, *81*, 3684.

(71) Ryckaert, J. P.; Ciccotti, G.; Berendsen, H. J. C. *J. Comput. Phys*. **1977**, *23*, 327.

(72) Essmann, U.; Perera, L.; Berkowitz, M. L.; Darden, T.; Lee, H.; Pedersen, L. G. *J. Chem. Phys*. **1995**, *103*, 8577.

(73) Kollman, P. A.; Massova, I.; Reyes, C.; Kuhn, B.; Huo, S.; Chong, L.; Lee, M.; Lee, T.; Duan, Y.; Wang, W.; Donini, O.; Cieplak, P.; Srinivasan, J.; Case, D. A.; Cheatham, T. E., III. *Acc. Chem. Res.* **2000**, *33*, 889.

(74) Still, W. C.; Tempczyk, A.; Hawley, R. C.; Hendrickson, T. *J. Am. Chem. Soc.* **1990**, *112*, 6127.

(75) Weiser, J.; Shenkin, P. S.; Still, W. C. *J. Comput. Chem*. **1999**, *20*, 217.

(76) Gilson, M. K.; Sharp, K. A.; Honig, B. H. *J. Comput. Chem*. **1988**, *9*, 327.

(77) Jayaram, B.; Sharp, K. A.; Honig, B. H. *Biopolymers* **1989**, *28*, 975.

(78) Sanner, M. F.; Olson, A. J.; Spehner, J. C. *Biopolymers* **1996**, *38*, 305.

(79) McQuarrie, D. A. A. *Statistical Mechanics*; Harper & Row: New York, 1976.

(80) Brooks, B. R.; Jan_e_zic, D.; Karplus, M. *J. Comput. Chem*. **1995**, *16*, 1522.

(81) Zhan, C.-G.; Dixon, D. A. *J. Phys. Chem. A* **2001**, *105*, 11534. (b) Zhan, C.-G.; Dixon, D. A. *J. Phys. Chem. A* **2002**, *106*, 9737. (c) Zhan, C.-G.; Dixon, D. A. *J. Phys. Chem. B* **2003**, *107*, 4403. (d) Zhan, C.-G.; Dixon, D. A. *J. Phys. Chem. A* **2004**, *108*, 2020.

(82) Kwong, P. D.; Wyatt, R.; Robinson, J.; Sweet, R. W.; Sodroski, J.; Hendrickson, W. A. *Nature* **1998**, *393*, 648.

(83) Olshevsky, U.; Helseth, E.; Furman, C.; Li, J.; Haseltine, W.; Sodroski, J. *J. Virol.* **1990**, *64*, 5701.

(84) Kwong, P. D.; Doyle, M. L.; Casper, D. J.; Cicala, C.; Leavitt, S. A.; Majeed, S.; Steenbeke, T. D.; Venturi, M.; Chaiken, I.; Fung, M.; Katinger, H.; Parren, P. W.; Robinson, J.; Van Ryk, D.; Wang, L.; Burton, D. R.; Freire, E.; Wyatt, R.; Sodroski, J.; Hendrickson, W. A.; Arthos, J. *Nature* **2002**, *420*, 678.

(85) Myszka, D. G.; Sweet, R. W.; Hensley, P.; Brigham-Burke, M.; Kwong, P. D.; Hendrickson, W. A.; Wyatt, R.; Sodroski, J.; Doyle, M. L. *Proc. Natl. Acad. Sci. U.S.A.* **2000**, *97*, 9026.